Journal of Power Sources 196 (2011) 2699–2708

Contents lists available at ScienceDirect

Journal of Power Sources

journal homepage: www.elsevier.com/locate/jpowsour

Performance of composite Nafion/PVA membranes for direct methanol fuel cells

Sergio Mollá [b], Vicente Compañ [a,b,*]

[a] Dpto. Termodinámica Aplicada, ETSII, Universidad Politécnica de Valencia, 46022 Valencia, Spain
[b] Instituto de Tecnología Energética (ITE), Avenida Juan de la Cierva 24, Paterna, 46980 Valencia, Spain

ARTICLE INFO

Article history:
Received 12 May 2010
Received in revised form 6 September 2010
Accepted 7 November 2010
Available online 12 November 2010

Keywords:
DMFC
Methanol permeability
Nanocomposite Nafion® membranes
PVA
Nanofibers

ABSTRACT

This work has been focused on the characterization of the methanol permeability and fuel cell performance of composite Nafion/PVA membranes in function of their thickness, which ranged from 19 to 97 μm. The composite membranes were made up of Nafion® polymer deposited between polyvinyl alcohol (PVA) nanofibers. The resistance to methanol permeation of the Nafion/PVA membranes shows a linear variation with the thickness. The separation between apparent and true permeability permits to give an estimated value of 4.0×10^{-7} cm^2 s^{-1} for the intrinsic or true permeability of the bulk phase at the composite membranes. The incorporation of PVA nanofibers causes a remarkable reduction of one order of magnitude in the methanol permeability as compared with pristine Nafion® membranes. The DMFC performances of membrane–electrode assemblies prepared from Nafion/PVA and pristine Nafion® membranes were tested at 45, 70 and 95 °C under various methanol concentrations, i.e., 1, 2 and 3 M. The nanocomposite membranes with thicknesses of 19 μm and 47 μm reached power densities of 211 mW cm^{-2} and 184 mW cm^{-2} at 95 °C and 2 M methanol concentration. These results are comparable to those found for Nafion® membranes with similar thickness at the same conditions, which were 210 mW cm^{-2} and 204 mW cm^{-2} respectively. Due to the lower amount of Nafion® polymer present within the composite membranes, it is suggested a high degree of utilization of Nafion® as proton conductive material within the Nafion/PVA membranes, and therefore, significant savings in the consumed amount of Nafion® are potentially able to be achieved. In addition, the reinforcement effect caused by the PVA nanofibers offers the possibility of preparing membranes with very low thickness and good mechanical properties, while on the other hand, pristine Nafion® membranes are unpractical below a thickness of 50 μm.

© 2010 Elsevier B.V. All rights reserved.

1. Introduction

Perfluorinated polyelectrolytes, such as Nafion®, are up to date the best proton conductors for low temperature fuel cells because of their combination of good chemical and mechanical stability in addition to relatively high conductivity of ca. 0.08 S cm^{-1} [1–4]. Though polymer electrolyte membranes (PEMs) for fuel cells are promising candidates for transportation, distributed power, and portable power applications, important scientific, technical and economical problems need to be solved before commercialization is possible.

Direct methanol fuel cells (DMFCs) are promising candidates as power generators for portable devices. Easy refuelling and high energy storage capacity are their main advantages. However, it is known that the use of Nafion® membranes in DMFCs causes problems such as methanol crossover, which entails the utilization of very thick membranes, and thus performance is reduced [5,6].

Recently, extensive work has been focused on Nafion® membranes modified with conducting polymers, such as polyaniline [7], polyaniline/silica [8] and polypyrrole [9], paying special attention to the methanol crossover in the composite membranes. It is worth noting that the mix of electronic conductivity of polyaniline with the ionic conductivity of cation-exchange membranes has also promoted the study of these composites for electrode modifications [10–14]. Mauritz et al. [15,16] demonstrated that hybrid Nafion/silica membranes in PEM applications produce advantages such as higher water uptake, lower methanol uptake, and greater mechanical strength than unmodified Nafion®. Sorption studies showed that the Nafion/silica membranes had a larger affinity for water over methanol, whereas the order is reversed for unmodified Nafion®. Consequently, these experimental results suggest that the methanol permeability through the hybrid membranes will be smaller than in unmodified membranes [17–19]. However, the improvement in lowering methanol penetrability of the new membranes always leads to the decrease in the proton conductivity.

* Corresponding author at: Dpto. Termodinámica Aplicada, ETSII, Universidad Politécnica de Valencia, Camino de Vera s/n, 46022 Valencia, Spain.
Tel.: +34 963879328; fax: +34 963877924.
E-mail address: vicommo@ter.upv.es (V. Compañ).

0378-7753/$ – see front matter © 2010 Elsevier B.V. All rights reserved.
doi:10.1016/j.jpowsour.2010.11.022

In this context, the synthesis of efficient solid electrolytes separating the anode from the cathode together with the development of cheaper catalysts for fuel oxidation are the main issues facing the development of commercial low temperature DMFCs. In principle, proton conducting ionic fillers would have a dual function: enhancement of the water retention and increase of the ion-exchange capacity (IEC) of the membranes, two properties that increase the proton conductivity. In membranes with high IEC, segregation of nanosize hydrophilic domains from the hydrophobic ones to form percolation paths for proton transport may be relatively easy. It is possible to think that ionic inorganic fillers trapped in hydrophobic domains separating hydrophilic domains might provide additional pathways for proton transport [20–22].

The purpose of this paper is to evaluate the methanol crossover and DMFC performance of novel nanocomposite membranes obtained by impregnation of nanofibers of polyvinyl alcohol (PVA) with a Nafion® solution. PVA is a polymer with a methanol permeability two orders of magnitude lower than Nafion®, and the nanofibers have been obtained by electrospinning of a water solution of the PVA polymer. The external surface of such PVA nanofibers has been functionalized with sulfonic acid groups in order to contribute to keep the high proton conductivity of Nafion®, while the PVA phase performs as a barrier for the transport of methanol across the membrane. Another advantage derived from the nanofibers is the mechanical reinforcement, which allows obtaining composite films much thinner than the commercial Nafion 117. The thickness of the composite membranes prepared in our laboratory ranged from 19 ± 1 μm to 97 ± 5 μm, with the aim of lowering the resistance to the transport of protons.

In this work we report the performance of the membrane electrode assemblies (MEAs) prepared from composite membranes of Nafion/PVA investigated through polarization curves at different temperatures and methanol concentrations. For comparison, Nafion® membranes presenting similar thicknesses have been prepared by the casting method and their performance analyzed. The differences observed between the membranes are discussed, paying special attention on methanol concentration, temperature and membrane thickness.

2. Experimental

2.1. Materials

A commercial 20 wt% Nafion® dispersion (DuPont Co.) was solvent exchanged in order to prepare a 5 wt% dispersion in isopropanol/water mixture, 4:1 w/w respectively.

Polyvinyl alcohol, PVA Mowiol 28-99 grade, was kindly supplied by the company Kuraray Europe GmbH.

Isopropanol extra pure and cetyltrimethylammonium bromide (CTAB) were purchased from Acros Organics, and 4-formyl-1,3-benzenedisulfonic acid disodium salt from Sigma–Aldrich.

2.2. Preparation of the membranes

2.2.1. Nafion® membranes

The solvent exchanged solution, with a 5 wt% Nafion® content in isopropanol and water, was used for the casting of pristine Nafion® membranes with thickness between 18 and 95 μm. The respective Nafion® membranes were annealed at 125 °C for 90 min in the oven and then removed from their petri glass dishes by adding water.

The last step was the conditioning of the membranes by treatment with hot hydrogen peroxide and chlorhydric acid solutions. Finally, the cast Nafion® membranes were washed with hot water, dried and stored.

2.2.2. PVA nanofiber reinforced Nafion® membranes

Porous PVA mats were produced by a standard electrospinning setup (Yflow S.L., Málaga, Spain) through the feeding of an aqueous solution of PVA (0.005:1:10 wt. CTAB:PVA:water). CTAB was used as surfactant in order to reduce surface tension of water and improve electrospinning ability.

A potential difference of 16 kV was applied between the needle and the planar collector, which were separated 25 cm, and a flow rate of 0.5 ml h^{-1} was used for the electrospinning process.

The collected mats were heated during 3 h at 170 °C in a vacuum atmosphere (250 mbar pressure) with the purpose of removing water and increasing manipulability.

The PVA mats were then mounted on a round steel frame and immersed into a bath in which the disodium salt of the 4-formyl-1,3-benzenedisulfonic acid was solved by a mixture of isopropanol/water (70/30 v/v), incorporating chlorhydric acid as a catalyst for the acetal reaction, which was carried out at 60 °C for 2 h. The sodium ions were exchanged with protons by means of a chlorhydric acid solution:

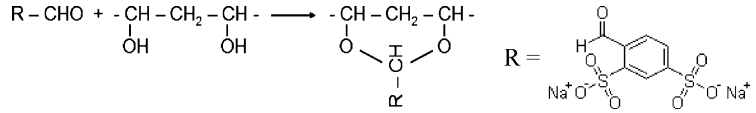

(1)

Subsequently, the PVA chains were crosslinked in order to raise mechanical, chemical and thermal properties of the nanofibers. This was accomplished by reaction with glutaraldehyde vapor in a closed vessel during 24 h at room temperature. After the crosslinking process, the mats were heated at 100 °C for 15 min with the aim to remove adsorbed glutaraldehyde and water.

Finally, the treated mats were impregnated with the prepared 5 wt% Nafion® dispersion in isopropanol/water 4:1 w/w. This ratio has been previously reported to be suitable for Nafion® infiltration into porous membranes [23]. Each impregnation step was carried out by wetting the PVA mat into the Nafion® dispersion for 5 min and followed by evaporation in an oven at 100 °C for 5 min more. This was repeated 8 times in every mat so that an outer visible Nafion® layer was formed.

Afterwards, the composite membranes were annealed at 125 °C for 90 min under pressure and then conditioned with hot aqueous solutions of hydrogen peroxide and chlorhydric acid, washed with hot water, dried and stored.

2.3. Characterizations of membranes

2.3.1. Coefficients of methanol permeability

In order to determine the methanol permeability coefficient through the composite membranes, an experimental setup as shown in Fig. 1 was used. Chamber A was filled with a 2 M aqueous solution of methanol, while chamber B was filled with water. Both chambers were kept under stirring and thermostatized at 70 °C. A sample of 500 μl from chamber B was taken every certain time and then introduced into a vial containing 500 μl of water. The composition of the vial content was analyzed by gas chromatography (GC, HP Co. model 8590A) with a capillary column (Agilent Co., 30 m × 0.53 mm × 20 μm) and a TCD detector. Seven patron solutions were previously prepared in order to obtain a calibration curve representing peak areas versus methanol concentrations.

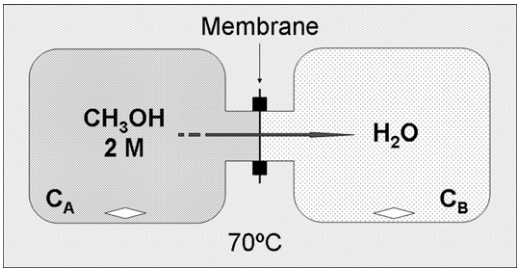

Fig. 1. Schematic representation of the experimental setup for the determination of the methanol permeability across the membranes.

The diffusion process of methanol across a membrane, in the stationary state, is described by the Fick's first law:

$$J = -D\frac{\partial C^{m}}{\partial x} = D\frac{\Delta C^{m}}{L} \tag{2}$$

where ΔC^{m} represents the variation in methanol concentration between the right and left sides of the membrane, with a thickness L, and can be expressed as $C_B - C_A$.

However, from a strict point of view, the methanol concentrations at both sides of the membrane, C_B^m and C_A^m, cannot be considered the same as the concentrations in bulk solution, since this transfer process is governed by the methanol solubility in such a membrane. Thus, we can define the membrane partition coefficient K as,

$$K = \frac{C_A^m}{C_A} = \frac{C_B^m}{C_B} \tag{3}$$

and therefore, the variation in the methanol concentration across the membrane will be given by,

$$\Delta C^{m} = C_B^m - C_A^m = K(C_B - C_A) = K\Delta C \tag{4}$$

The flux of methanol J can also be expressed as the amount of methanol in moles n crossing the membrane (thickness L) per unit of time t and area A. We can rewrite the Fick's law as:

$$J = \frac{dn}{A\ dt} = DK\frac{\Delta C}{L} \tag{5}$$

where,

$$n = C_B V_B \rightarrow dn = V_B\ dC_B \tag{6}$$

Thus:

$$\frac{V_B\ dC_B}{A\ dt} = DK\frac{\Delta C}{L} \tag{7}$$

If we take into account that the difference in concentration between both sides of the membrane, $\Delta C = C_B - C_A$, is practically constant due to the fact that $C_A \gg C_B$, then:

$$dC_B = \frac{DKA}{LV_B}C_A\ dt \tag{8}$$

Integrating Eq. (8), the following expression is obtained:

$$C_B = \frac{DKA}{LV_B}C_A t \tag{9}$$

The product between the diffusion coefficient, D, and the membrane partition coefficients, K, measures the apparent permeability coefficient P:

$$P = DK \tag{10}$$

where, the name apparent means the permeability through the whole system (membrane + boundary layers) and not only to the membrane.

Combining Eqs. (9) and (10), we can obtain the final expression which shows how varies the concentration of methanol in chamber B as a function of time:

$$C_B = \frac{PA}{LV_B}C_A t \tag{11}$$

where, C_B: concentration of methanol in chamber B. C_A: concentration of methanol in chamber A (2 M), P: coefficient of apparent methanol permeability across the membrane ($cm^2\ s^{-1}$). A: area of the membrane (2.27 cm^2). L: thickness of the membrane (cm). V_B: volume of water which fills the chamber B (150 cm^3). t: time reached at each measurement (s).

If we plot C_B versus time, a straight line will be obtained of which slope m the apparent permeability can be calculated.

$$m = \frac{PA}{LV_B}C_A \tag{12}$$

The apparent transmissibility of methanol across the membrane system (membrane + boundary layers) is defined by the relation P/L. The inverse of the slope m is:

$$\frac{1}{m} = \frac{L}{P}\frac{V_B}{AC_A} \tag{13}$$

where the reciprocal of the apparent transmissibility, L/P, is related with the resistance of the total system to the methanol flux.

The total resistance of the system has two components: one derived from the intrinsic material properties of the membrane and other due to the boundary layers, that is, the transfer process between the bulk solution and the membrane surface [24].

$$\left(\frac{L}{P}\right)_{App} = \left(\frac{L}{P}\right)_{True} + R_{B.L.} \tag{14}$$

Thus, plotting the value of the resistance to the methanol flux $(L/P)_{App}$ calculated for each membrane versus its membrane thickness (L) will develop a straight line of which slope, equivalent to $1/P_{True}$, can be calculated by the true methanol permeability coefficient of the membrane (P_{True}).

2.3.2. MEA preparation

Composite membranes based on Nafion® and PVA nanofibers, as well as pristine Nafion® membranes, were used for the preparation of membrane electrode assemblies (MEAs) in order to study their DMFC performance.

The anode and cathode electrodes used for MEA preparation were acquired from Baltic Fuel Cells GmbH (Schwerin, Germany). The anode was composed of a carbon paper gas diffusion layer (GDL) from Freudenberg & Co. (Weinheim, Germany), model H2315 T105A, covered by an alloy of Pt–Ru black 50:50 (Alfa Aesar) with a catalyst loading of 5.0 mg cm^{-2} together with a 20 wt% of dry Nafion® ionomer. Similarly, the cathode was composed of a GDL from Freudenberg & Co., model H2315 I3C4, with a catalyst loading of 5.0 mg cm^{-2} of platinum nanoparticles supported by advanced carbon (HiSPEC 13100, Alfa Aesar) with a Pt/C ratio of 70 wt%, and the electrode also contained a 20 wt% of dry Nafion® ionomer.

2.3.3. DMFC performance of composite Nafion/PVA and Nafion® membranes

The MEAs were previously equilibrated with water and then placed into a single fuel cell hardware with a square 5 cm^2 active area (quick CONNECT, Baltic Fuel Cells GmbH), containing graphite serpentine flow fields and equipped with a pressure-controlled clamping force system.

Different concentrations of aqueous methanol solution, i.e. 1 M, 2 M and 3 M, were pumped at a flow rate of 5 ml/min to feed the anode. The cathode was directly fed with oxygen gas at a flow rate of 150 ml/min and atmospheric pressure.

Table 1
Thickness, water uptake at 70 °C, ionic exchange capacity and proton conductivity at 95 °C and fully hydrated conditions for composite Nafion/PVA. Nafion® is included for comparison.

Membrane	Thickness (μm)	Water uptake (%)	IEC (meq g^{-1})	λ (mol H_2O)/(mol SO_3H)	$\sigma^{95\,°C}$ (S cm^{-1})
Nafion/PVA	19 ± 1	26.4 ± 0.1	0.47 ± 0.1	42	0.012
Nafion/PVA	26 ± 2	19.3 ± 0.1	0.33 ± 0.1	44	0.012
Nafion/PVA	39 ± 3	27.9 ± 0.1	0.45 ± 0.1	47	0.016
Nafion/PVA	47 ± 3	25.8 ± 0.1	0.58 ± 0.1	34	0.025
Nafion/PVA	61 ± 3	22.9 ± 0.1	0.57 ± 0.1	30	0.010
Nafion/PVA	97 ± 5	35.8 ± 0.1	0.55 ± 0.1	49	0.007
Nafion®	18 ± 1	27.0 ± 0.1	0.93 ± 0.1	22	0.015
Nafion®	28 ± 1	27.0 ± 0.1	0.93 ± 0.1	22	0.027
Nafion®	37 ± 1	27.0 ± 0.1	0.93 ± 0.1	22	0.034
Nafion®	46 ± 1	27.0 ± 0.1	0.93 ± 0.1	22	0.035
Nafion®	60 ± 2	27.0 ± 0.1	0.93 ± 0.1	22	0.049
Nafion®	95 ± 2	27.0 ± 0.1	0.93 ± 0.1	22	0.070
Nafion 117 (commercial)	216 ± 4	21.5 ± 0.1	0.91 ± 0.1	18	0.096

I–V polarization curves (current density versus potential) were obtained at several temperatures, i.e. 45 °C, 70 °C and 95 °C, from open circuit voltage (OCV) conditions up to 0.2 V by stepwise increment of the current density. Power density values were thus calculated and represented. Before *I–V* measurements, the MEAs were activated for 5 h to enhance their performance.

3. Results and discussion

3.1. Properties of the Nafion/PVA membranes

Table 1 summarizes thickness, water uptake, ion-exchange capacity (IEC) and conductivity of the composite Nafion/PVA membranes. A detailed procedure for the preparation and characterization of the composite Nafion/PVA membranes has been previously described by the authors [25]. Nafion® membranes have also been included for comparison, and as also reported, their conductivity was found to be linearly thickness-dependent [25].

The absolute values for the water uptake at 70 °C of the Nafion/PVA membranes are similar to those of pristine Nafion® membranes prepared in our laboratory by casting and slightly higher than the value obtained for commercial Nafion 117. However, the λ values, which relate the molar content of water molecules to the total number in moles of sulfonic acid groups within the membrane, show values between 18 and 22 for the pristine Nafion® materials, as expected since Nafion® saturates at λ = 22, whereas the nanocomposite Nafion/PVA membranes show much larger values. This observation would suggest that the PVA nanofibers within the composite membranes are also swelling in a certain degree due to the strong hydrophilic character of the PVA molecule.

Ion-exchange capacities of the Nafion/PVA membranes are nearly the half of the typical values observed for pure Nafion® materials, assumed to be due to the replacement of Nafion® polymer by the PVA nanofiber phase. Consequently, the conductivity measurements have also reflected lower values as compared to pristine Nafion®.

An explanation of this behaviour is assumed to be due to the only superficial functionalization of the PVA nanofibers, which hardly influenced the total ion-exchange capacity (IEC) of the membrane, and therefore, the IEC has been lowered by the PVA presence and the conductivity has been reduced. However, it has been desired just to functionalize the surface of the nanofibers in order to keep the barrier properties showed by the bulk PVA. If the PVA would have been fully sulfonated, the methanol crossover across its volume would have strongly increased, and therefore, the nanofiber phase would have not showed barrier properties against methanol.

The composite membrane with a thickness of 47 μm showed the maximum proton conductivity at the whole studied temperature range, achieving 0.025 S cm^{-1} at 95 °C and fully hydrated conditions.

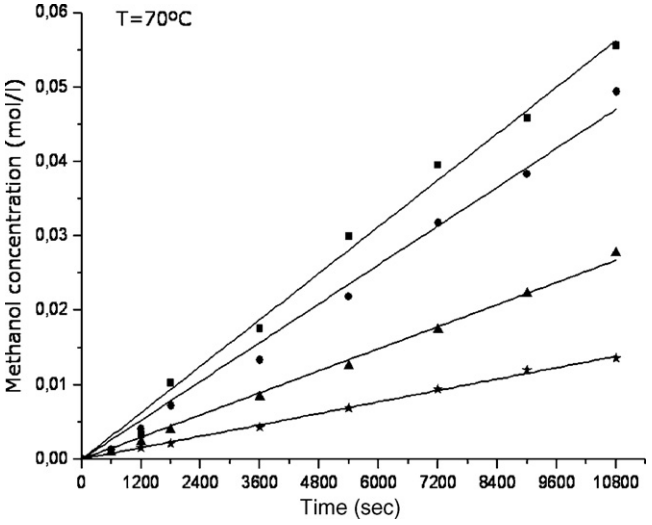

Fig. 2. Methanol concentration (C_B) versus time at the permeability experiments for composite Nafion/PVA membranes with different thicknesses. (■) 26 μm, (●) 39 μm, (▲) 61 μm, (★) 97 μm.

3.2. Apparent and true methanol permeabilities across the composite membranes

It has been characterized the methanol transport across Nafion/PVA membranes with different thicknesses by means of the setup already described in Fig. 1. The temperature of the bath was fixed at 70 °C and chamber A was filled with a 2 M methanol solution.

Samples (500 μl) from chamber B were taken within a period between 0 and 3 h, i.e. 600 s, 1200 s, 1800 s, 3600 s, 5400 s, 7200 s, 9000 s and 10,800 s. These were analyzed by gas chromatography and their chromatograms compared with the calibration curve, correlating the chromatograms peak areas with methanol concentrations.

Fig. 2 depicts the variation of methanol concentration in chamber B versus time. Straight lines with different slopes ($m = C_B/t$) have been obtained as a function of the membrane thickness. By application of Eq. (1) with the experimental parameters and the values of the obtained slopes, the apparent methanol permeability of the membranes can be calculated.

Table 2 shows the apparent permeability coefficients obtained for Nafion/PVA membranes and are compared with those reported for a cast Nafion® membrane, prepared with a similar dispersion

Table 2
Apparent methanol permeabilities (P_{App}) at 70 °C for several composite Nafion/PVA membranes and for cast and commercial Nafion® membranes.

Membrane	Thickness (μm)	Slope (C_B/t) (mol l^{-1} s^{-1})	P_{App} methanol (cm^2 s^{-1})
Nafion/PVA	26 ± 2	5.21295×10^{-6}	4.13×10^{-7}
Nafion/PVA	39 ± 3	4.35606×10^{-6}	5.33×10^{-7}
Nafion/PVA	61 ± 3	2.47526×10^{-6}	4.99×10^{-7}
Nafion/PVA	97 ± 5	1.28308×10^{-6}	4.11×10^{-7}
Nafion[a] [26]	175	–	5.58×10^{-6}
Nafion N117 [26]	178	–	4.36×10^{-6}

[a] Cast membrane using Nafion® dispersion in isopropanol/water (4:1 w/w). C_B measured by densimetry.

composition, and for a commercial Nafion 117 membrane. With the purpose of obtaining the true or intrinsic permeability of the membranes Nafion/PVA, it has been plotted the reciprocal of the transmissibility of the membranes, that means the resistance that the membrane offers to methanol flux, L/P, as a function of the membrane thickness (Fig. 3).

The value of the true methanol permeability, P_{True}, is obtained from the reciprocal of the slope of the straight-line plotted in Fig. 3, $m = (2.196 \pm 0.195) \times 10^6$. This parameter represents an intrinsic property of the material and a value of $(4.55 \pm 0.40) \times 10^{-7}$ cm^2 s^{-1} has been calculated for the Nafion/PVA membranes.

These results of methanol permeability for the nanocomposite membranes prepared in our work are very promising and validate the capacity of the PVA nanofibers to perform as barriers for the methanol diffusion. It is worth noting that the intrinsic methanol permeability coefficient of the Nafion/PVA membranes are one order of magnitude below the permeabilities at 70 °C for Nafion® membranes prepared by casting in our laboratory, as well as much lower than the typical permeability coefficients reported for commercial Nafion 117 membranes at room temperature $(2.3 \pm 0.2) \times 10^{-6}$ cm^2 s^{-1}, according to the literature [27–30].

3.3. Performance of MEAs in direct methanol fuel cell operation

Figs. 4 and 5 are graphically represented data of the cell potential, V, and power density curves versus current density, I, for the MEAs prepared with pristine Nafion® membranes (thicknesses of 18 μm and 46 μm) and composite Nafion/PVA membranes (19 μm and 47 μm), when DMFC was operated at 45, 70 and 95 °C, and fed with 1, 2 and 3 M of methanol solutions.

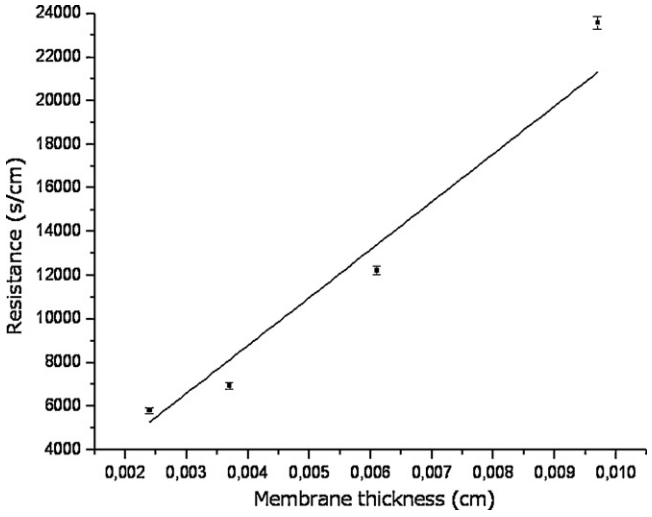

Fig. 3. Representation of the resistance to the methanol permeation across the Nafion/PVA membranes as a function of their thickness.

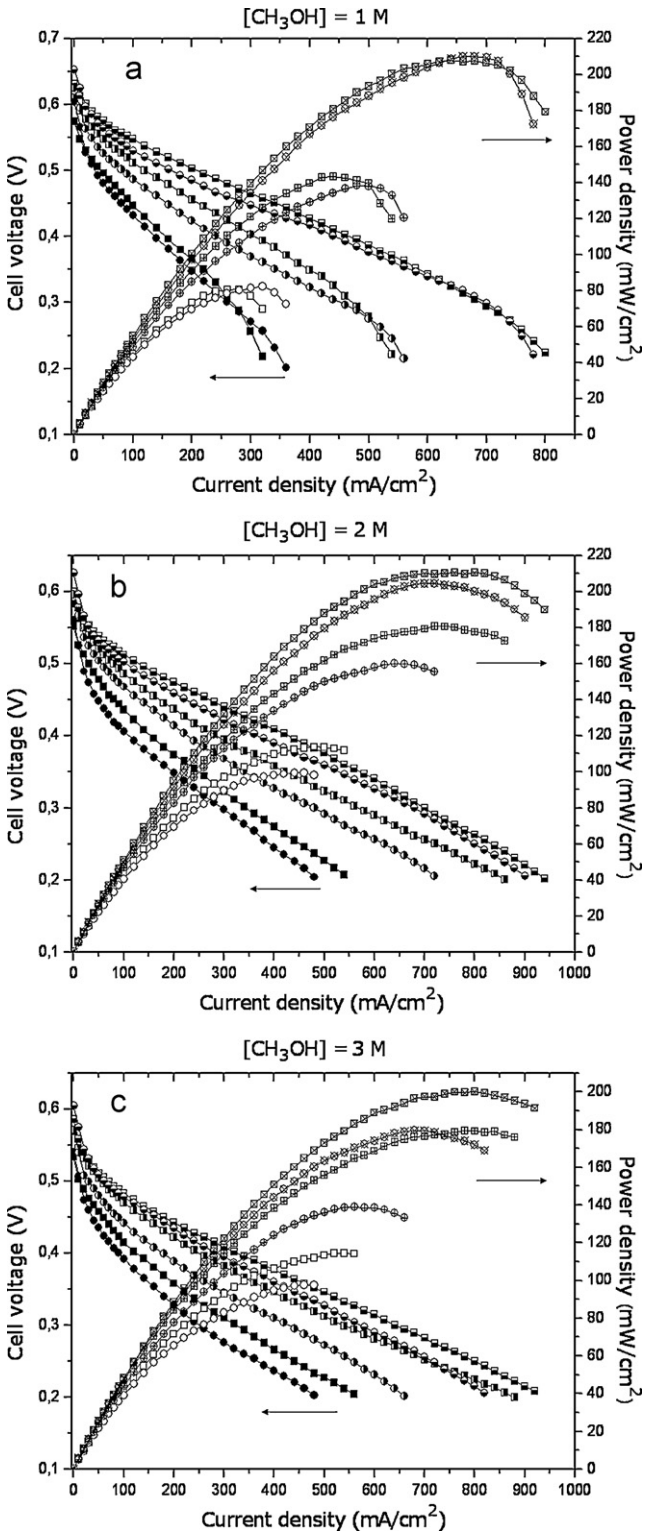

Fig. 4. *I–V* and power density curves for pristine Nafion® membranes at different conditions of temperature and thickness (■,□) 45 °C – 18 μm, (◨,⊞) 70 °C – 18 μm, (◪,⊠) 95 °C – 18 μm, (●,○) 45 °C – 46 μm, (◑,⊕) 70 °C – 46 μm, (◒,⊗) 95 °C – 46 μm, and by feeding methanol solutions with (a) 1 M, (b) 2 M, and (c) 3 M concentrations.

The cell potential at OCV conditions ($I = 0$) usually does not reach the theoretical value of the overall reversible cathode and anode potential at the given pressure and temperature. The drop of the OCV from the theoretical voltage has been attributed to the penetration of the fuel across the membrane, and thus, these values are

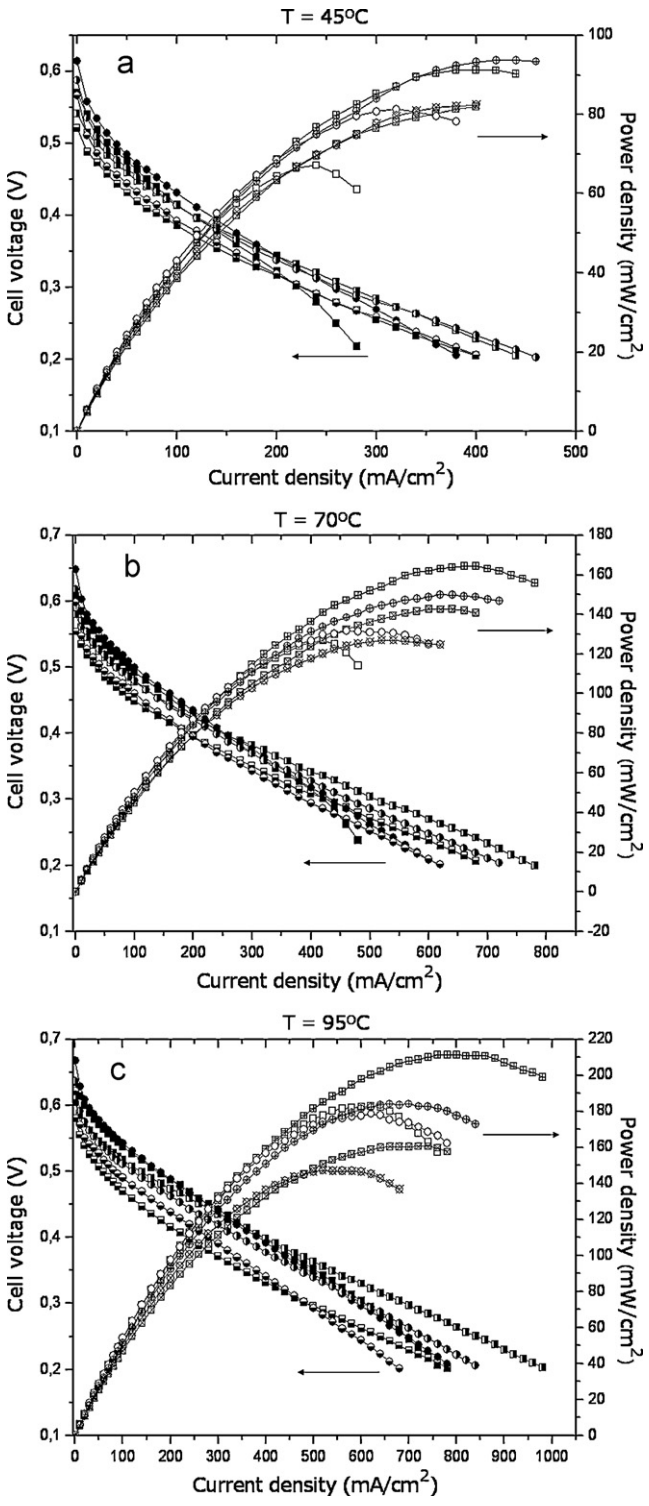

Fig. 5. *I–V* and power density curves for composite Nafion/PVA membranes at different conditions of methanol concentration and thickness (■,□) 1 M – 19 μm, (◨,⊞) 2 M – 19 μm, (⬓,⊠) 3 M – 19 μm, (●,○) 1 M – 47 μm, (◑,⊕) 2 M – 47 μm, (◒,⊗) 3 M – 47 μm, and by fixing a cell temperature of (a) 45 °C, (b) 70 °C, and (c) 95 °C.

a good indicator of the degree of methanol crossover by diffusion [31].

Table 3 summarizes the OCV values of MEAs prepared with Nafion® and composite Nafion/PVA membranes fed by 1, 2 and 3 M methanol solutions at 45, 70 and 95 °C. Those OCV values decrease in all cases with the increase in methanol concentration, due to a larger fuel permeation, while at a fixed methanol concentration, the values of OCV increase with the temperature favored by the accelerated electrochemical reactions. These results obtained indicate that the effect of the activation energy in the electrochemical reaction (voltage increment) is higher than the opposite effect caused by the increased methanol crossover (voltage reduction), and thus, the combined effect is only a moderate increase of the cell potential with the temperature.

Table 3
Values for the open circuit voltage (OCV) condition obtained for membranes at different conditions of temperature and methanol concentration.

Membrane	L (μm)	OCV (V)			$[CH_3OH]$ (M)
		45 °C	70 °C	95 °C	
Nafion/PVA	19 ± 1	0.570	0.608	0.635	1
		0.541	0.580	0.604	2
		0.521	0.554	0.580	3
Nafion®	18 ± 1	0.574	0.610	0.631	1
		0.552	0.583	0.600	2
		0.534	0.569	0.586	3
Nafion/PVA	47 ± 3	0.614	0.648	0.668	1
		0.587	0.618	0.637	2
		0.566	0.598	0.621	3
Nafion®	46 ± 1	0.604	0.625	0.653	1
		0.560	0.596	0.626	2
		0.540	0.571	0.605	3
Nafion 117	216 ± 4	0.673	0.688	0.708	1
		0.650	0.653	0.668	2
		0.624	0.653	0.673	3

However, at a fixed temperature and methanol concentration, the OCV follows the trend Nafion (18 μm) ≈ Nafion/PVA (19 μm) < Nafion (46 μm) < Nafion/PVA (47 μm) < Nafion 117. At very low thicknesses, Nafion® and Nafion/PVA behave very similar, while at medium size thicknesses, Nafion/PVA exceeds pristine Nafion®. Commercial Nafion 117 is a very large thickness membrane, and therefore, its OCV values comprise the higher levels.

It would really be expected that the comparison between membranes of pristine Nafion® and Nafion/PVA with similar thickness would show higher OCV values for the composite ones as a more reduced methanol crossover is reported. However, not only the methanol crossover is known to be responsible on the OCV parameter. Another factors as homo/heterogeneity of the membrane and electrodes, catalyst loading, MEA preparation, water management and blocking of pores in gas diffusion layers, catalytic activity and reaction kinetics, proton conductivity, gradient of methanol concentration within the catalytic layer, porosity of gas diffusion and catalytic layers, air/oxygen flow rates, contact pressures, temperature, etc. can influence the OCV values. Unfortunately, all these parameters are difficult to control together.

For example, it has been reported that the ability of air/oxygen to reach the catalyst layer is a very important factor with regards to the OCV parameter, since the OCV values diminish due to the competitive reaction of methanol oxidation against oxygen reduction over the cathode catalyst, and thus it depends on the methanol crossover, but the available amount of oxygen, depending on the flow rate, strongly affects this reaction as well, and therefore, the OCV typically increases with the oxygen/air flow rate since more methanol is dissipated from the cathode [32].

It is also worth to mention that our composite membranes showed lower proton conductivity values than the pristine Nafion® membranes with similar thickness, and it has been reported by another authors that proton conductivity can influence the OCV values too, since from a practical point of view, the OCV values cannot be obtained at conditions of null intensity ($I = 0$), and at least $I = 0.01$ A is usually necessary. Thus, this factor must be also taken into account [33]. In fact, taking a look at Table 3 it is possible to remark that the Nafion/PVA membrane (47 μm) which showed the higher proton conductivity among the composite membranes

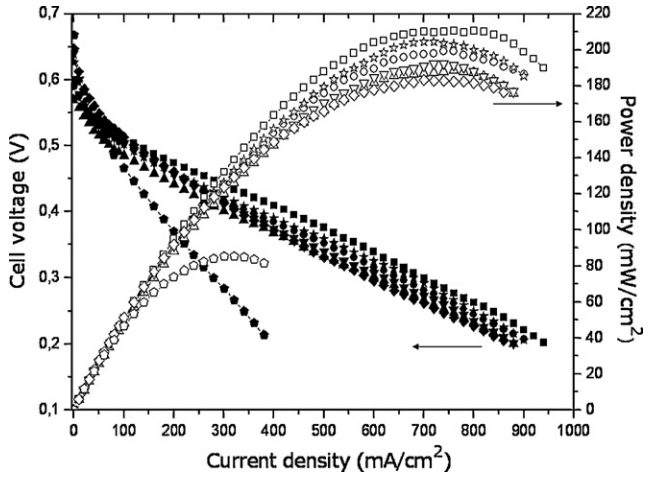

Fig. 6. DMFC performances at 95 °C and 2 M methanol solutions for pristine Nafion® membranes in relation to their thicknesses. (■) 18 μm, (▲) 28 μm, (●) 37 μm, (★) 46 μm, (▼) 60 μm, (♦) 95 μm, (⬟) 216 μm, commercial N117.

exceed the OCV values measured for the Nafion® membrane with comparable thickness (46 μm).

Fig. 4 clearly shows that performances follow the order 95 °C > 70 °C > 45 °C. The differences in performance, especially between 70 and 95 °C, become smaller when increasing methanol concentration. At 1 M, due to the low methanol concentration, the temperature effect is the most significant.

On the other hand, Fig. 5 elucidates an optimum methanol concentration at 2 M. Due to mass transport problems, 1 M concentration results are not convenient, although at 95 °C the performance with 1 M methanol solution surpasses that one showed by the 3 M concentration.

Figs. 6 and 7 represent the performances of the MEAs prepared with both pristine Nafion® and composite Nafion/PVA membranes ranging different thicknesses, at the conditions of 2 M methanol solution and 95 °C.

In the case of pristine Nafion® (Fig. 6), the maximum power density is achieved with the thinnest (18 μm) membrane, reaching 210 mW cm^{-2}, assumed to be due to its very low protonic resistance which greatly compensates the negative effect of the high flux of methanol permeating across. However, the 28 μm thickness membrane shows a lower performance, which might be attributed to the larger resistance while methanol flux still keeps being high. For the 37 and 46 μm membranes, performance increases with the thickness, and thus, the membrane of 46 μm thickness shows the second maximum power density, 204 mW cm^{-2}. A reasonable explanation of this phenomenon would suggest that membranes benefit of increasing thickness as a consequence of a methanol flux reduction, despite the protonic resistance increases proportionally to thickness.

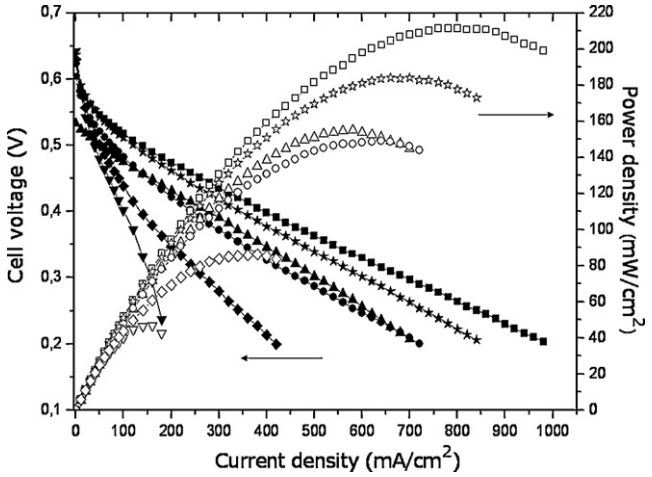

Fig. 7. DMFC performances at 95 °C and 2 M methanol solutions for composite Nafion/PVA membranes in relation to their thicknesses. (■) 19 μm, (▲) 26 μm, (●) 39 μm, (★) 47 μm, (▼) 61 μm, (♦) 97 μm.

The benefit on the methanol permeation caused by the effect of thickness applies up to 50 μm, and those membranes presenting thicknesses higher than that value show performances decreasing accordingly. In this sense, the membrane with 60 μm thickness has a performance similar to that one of 28 μm, and the 95 μm membrane slightly below those ones. The poorest performance has been found for the commercial Nafion 117 membrane, with a power density of 85 mW cm^{-2}, since it holds a very large thickness (216 μm at fully hydrated conditions) and thus undergoes an important protonic resistance, although on the other hand, its methanol permeation rate is the lowest as suggested by its OCV value.

Fig. 7 represents the performances of the prepared Nafion/PVA membranes. Again, the membranes with thicknesses of 19 and 47 μm show the best performances, 211 and 184 mW cm^{-2} respectively, which are almost similar to those ones showed by the Nafion® membranes of comparable thickness. As mentioned before, a thickness below 20 μm involves a very low protonic resistance and the best performance result. In the case of the Nafion/PVA membrane of 47 μm, Table 1 exhibits the largest conductivity value achieved, 0.025 S cm^{-1} at 95 °C under fully hydrated conditions, which combined with the intrinsically reduced methanol permeability would explain its very good performance.

The low conductivities found for the composite membranes when compared with Nafion® makes the protonic resistance to be the most significant parameter, and therefore, the effect of thickness has a more profound impact on the performance. Thus, the membranes with thickness larger than 50 μm performed very poor. With regard to this, the 97 μm membrane was found to perform better than the membrane of 61 μm thickness. The former was built by hot pressing of two thinner pieces of Nafion/PVA membrane, while the last one was prepared from a single PVA nanofiber mat. This experimental result suggests that large thickness PVA mats are not suitable for the infiltration of Nafion® polymer, since diffusion of the dispersion within the inner part of the porous mat should become more restricted.

A close inspection on the *I*–*V* curves (Figs. 4–7) shows two different regions: region-I, in which the activation process of the MEA occurs, is characteristic of low current densities; and region-II, typically at current densities *I* above 100 mA cm^{-2}, is characterized by showing a linear negative slope. The latter region is dominated by the protonic resistance of the membrane and its methanol crossover, which can be attributed to mechanisms of diffusion and electro-osmosis [34–36].

The cell voltage of a DMFC can be written as [31],

$$V = E - A_1 \quad \ln\left(\frac{I}{I_0}\right) - \frac{IL}{\sigma} - \eta_{cros} \tag{15}$$

where V is the cell voltage, E the reversible open circuit voltage, I the current density, I_0 the current density at which the overvoltage begins to move from zero, A_1 the sum of the slopes of the polarization curves for anode and cathode, L is the thickness of the membrane clamped between the anode and cathode electrode layers, σ the conductivity of the membrane and η_{cros} is the overpotential produced by methanol crossover.

The methanol crossover causes depolarization losses at cathode, by competitive reaction with oxygen, and concentration losses in anode as fuel permeates. The overpotential due to the

methanol crossover, η_{cros}, can be calculated following the procedure described by Huang et al. [36], by mean of the expression:

$$\eta_{cros} = \chi J_{MeOH} = \chi(J_{con} + IJ_{cros}) \quad (16)$$

where χ is a constant and J_{MeOH} the flux of methanol crossing the membrane. This flux has a current independent term affected by methanol concentration C_{an} at anode, i.e. J_{con}, and a current dependent term due to electro-osmosis of methanol, i.e. J_{cros}.

Substituting Eq. (16) into Eq. (15), we obtain,

$$V = E - A_1 \ln\left(\frac{I}{I_0}\right) - \frac{IL}{\sigma} - \chi(J_{con} + IJ_{eos}) \quad (17)$$

Assuming a Ficken diffusion and a linear concentration gradient across the thickness direction of the membrane, i.e. diffusion coefficient is independent of the concentration differential between anode and cathode sides, and the methanol molecules penetrating from anode and cathode are catalytically oxidized. Thus, J_{con} becomes a dependent term of the methanol concentration in anode,

$$J_{con} = kC_{an} \quad (18)$$

being k a constant which depends on the methanol diffusivity across the membrane. Substituting Eq. (19) into Eq. (17), rearranging Eq. (18) and separating the C_{an}-dependent and I-dependent terms, it results the following expression:

$$V(I, C_{an}) = E - A_1 \ln\left(\frac{I}{I_0}\right) - A_2 C_{an} - A_3 I \quad (19)$$

with

$$A_2 = \chi k \quad (20)$$

$$A_3 = \frac{L}{\sigma} + \chi J_{eos} \quad (21)$$

where A_2 is a term relating the overvoltage to the methanol crossover by diffusion, A_3 is a term relating the overvoltage influenced by the sum of the protonic resistance and the methanol electro-osmotic effects. These equations are only valid in the region-II of I–V curves. The derivative dV/dI when the concentration of the methanol in the anode is constant, is equal to,

$$\frac{dV}{dI} = -\frac{A_1}{I} - A_3 \quad (22)$$

At current densities above 100 mA cm^{-2}, $(A_1/I) < (A_1/100) \ll A_3$. Thus, A_3 can be obtained from the slope of the plot of V versus I at a fixed temperature as well as methanol feed concentration C_{an} and $I > 100$ mA cm^{-2}.

Fig. 8 shows the variation of the cell voltage, V, versus I for MEAs prepared with Nafion® and Nafion/PVA membranes of thickness between 46 and 47 μm operated at 70 °C and 95 °C with methanol feed concentrations of 1 M, 2 M and 3 M. Since A_3 relates the overvoltage to a combination of protonic resistance, i.e. L/σ, and methanol crossover by electro-osmosis, i.e. χJ_{eos}, this latter parameter can be estimated by subtracting L/σ from A_3. In Table 4 we summarize the values of χJ_{eos} $(A_3 - L/\sigma)$ as a function of methanol concentration and temperature for different MEAs.

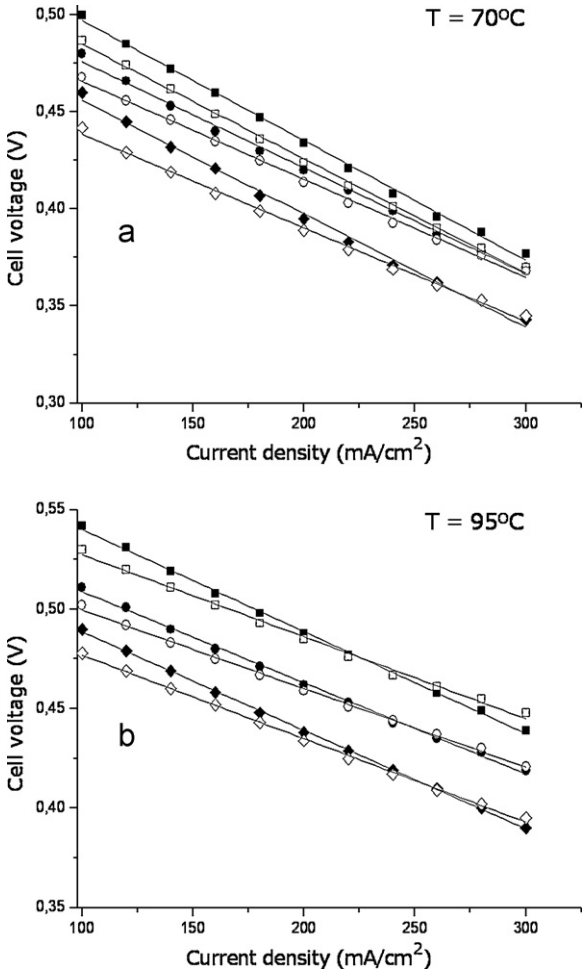

Fig. 8. Single cell voltage versus current density between 100 and 300 mA cm^{-2} for MEAs prepared from Nafion® (open symbol) and Nafion/PVA (filled symbol) operated at (a) 70 °C, and (b) 95 °C, with methanol feed concentrations of (square) 1 M, (circle) 2 M, and (rhombus) 3 M.

From this table it can be observed that χJ_{eos} decreases in the Nafion/PVA membrane in comparison with Nafion® at 70 °C and methanol concentrations of 1 M and 2 M. However, at the other conditions, χJ_{eos} tends to be similar for both Nafion® and Nafion/PVA membranes.

It is also remarkable to notice that the electro-osmotic drag effect becomes reduced with temperature. This behaviour has also been found by other authors [37]. However, Luo et al. have reported that electro-osmotic drag coefficient of water in Nafion® membrane raises with increasing temperature due to the higher amount of protons transported by diffusion with relation to those transported by the Grotthuss mechanism [38]. In the case of a methanol solution, the observed phenomena seem to indicate a weakening of the interaction between the proton and the methanol

Table 4
Parameter χJ_{eos} (V cm^2 mA^{-1}) for the electro-osmotic diffusion of methanol across Nafion/PVA and pristine Nafion® membranes.

[CH_3OH]	L (μm)	1 M	2 M	3 M	T (°C)
Nafion/PVA	19 ± 1	$(4.09 \pm 0.09) \times 10^{-4}$	$(2.82 \pm 0.10) \times 10^{-4}$	$(2.95 \pm 0.08) \times 10^{-4}$	70
		$(3.16 \pm 0.05) \times 10^{-4}$	$(2.41 \pm 0.06) \times 10^{-4}$	$(3.35 \pm 0.10) \times 10^{-4}$	95
Nafion®	18 ± 1	$(4.15 \pm 0.03) \times 10^{-4}$	$(3.37 \pm 0.08) \times 10^{-4}$	$(3.16 \pm 0.09) \times 10^{-4}$	70
		$(2.91 \pm 0.07) \times 10^{-4}$	$(2.39 \pm 0.05) \times 10^{-4}$	$(2.51 \pm 0.07) \times 10^{-4}$	95
Nafion/PVA	47 ± 3	$(4{,}03 \pm 0.11) \times 10^{-4}$	$(3{,}30 \pm 0.12) \times 10^{-4}$	$(3{,}69 \pm 0.14) \times 10^{-4}$	70
		$(3{,}25 \pm 0.07) \times 10^{-4}$	$(2{,}70 \pm 0.08) \times 10^{-4}$	$(3{,}07 \pm 0.04) \times 10^{-4}$	95
Nafion®	46 ± 3	$(4{,}48 \pm 0.09) \times 10^{-4}$	$(3{,}63 \pm 0.09) \times 10^{-4}$	$(3{,}40 \pm 0.10) \times 10^{-4}$	70
		$(2{,}80 \pm 0.10) \times 10^{-4}$	$(2{,}63 \pm 0.06) \times 10^{-4}$	$(2{,}88 \pm 0.06) \times 10^{-4}$	95

Table 5
Fitting parameters for the *I–V* curves of Nafion® and Nafion/PVA membranes which showed the best performances using 2 M methanol solutions at 70 °C and 95 °C conditions.

Membrane	L (μm)	E (V)	I_0 (mA cm^{-2})	A_1 (V)	A_3 (Ω cm^2)	T (°C)
Nafion/PVA	19 ± 1	0.580	2.368	1.319×10^{-2}	0.481	70
		0.604	1.229	9.778×10^{-3}	0.401	95
Nafion®	18 ± 1	0.583	1.618	1.118×10^{-2}	0.463	70
		0.600	0.636	9.562×10^{-3}	0.356	95
Nafion/PVA	47 ± 3	0.618	0.243	1.324×10^{-2}	0.546	70
		0.637	0.129	1.138×10^{-2}	0.459	95
Nafion®	46 ± 3	0.596	0.546	1.385×10^{-2}	0.505	70
		0.626	0.129	1.184×10^{-2}	0.395	95

molecule in relation to the proton–water molecule as the temperature increases.

Finally, we have fitted the experimental data of the *I–V* curves with a model based on Eq. (19), and thus, the parameters A_1, I_0 and A_2 have been estimated, while keeping E and A_3 fixed. For A_3, the values calculated for obtaining χJ_{eos} have been used. Table 5 summarizes the values of the cited parameters. A_2 has not been included since it resulted to be negligible in all the modelled experiments. Fig. 9 shows the fitting between some experimental and modelled curves, where it can be observed that Eq. (19) fits very well with the results of performance obtained at 2 M methanol concentration.

As usual, the open circuit voltage E sharply decreases from the thermodynamic electromotive force of the cell to a value in the vicinity of 0.58–0.64 V. This sharp decease is caused by internal currents, activation energy and, specially, by fuel crossover. The parameter A_3, which is related to the ohmic resistance of the membrane, decreases in each membrane as the temperature increases, due to the activation phenomenon of the protonic conductivity. These values of the ohmic resistance obtained from the polarization curves are in fair agreement with those measured directly by impedance spectroscopy in the MEAs built with the same membranes [25].

For a similar thickness and temperature, the Nafion/PVA membranes show higher values of A_3 in comparison with those of pristine Nafion®, since the composite membranes have lower protonic conductivity than the Nafion® membranes as expected by their reduced values of ion-exchange capacity (see Table 1). For each membrane, the parameters I_0 and A_1 also show a decrease as the temperature increases. Since both parameters are related with the catalytic activity of the catalyst layer at the electrodes, this would suggest that as the methanol crossover rises with the temperature, the specific active area of the catalyst should diminish as a consequence of the undesired reaction between the methanol and the oxygen.

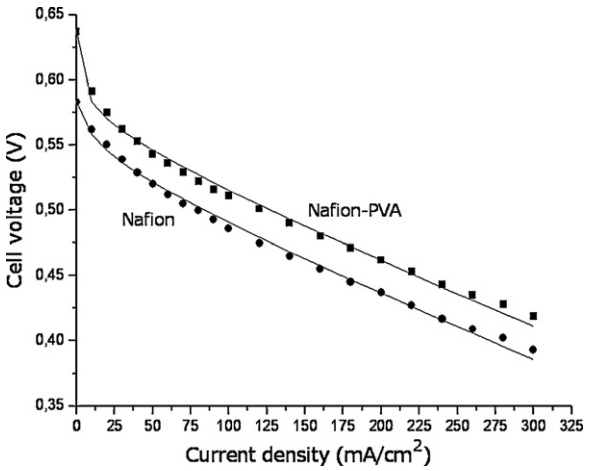

Fig. 9. Fitting between experimental (solid) and modelled (line) data points for the obtained *I–V* curves of (●) a pristine Nafion membrane with thickness of 46 μm at 70 °C, and (■) a Nafion–PVA membrane of 47 μm at 95 °C.

4. Conclusions

Novel nanocomposite membranes made up of Nafion® polymer infiltrated between functionalized polyvinyl alcohol (PVA) nanofibers have been prepared and characterized regarding their methanol permeability and DMFC performance. It was found that the reinforcement effect caused by the PVA nanofibers enabled the preparation of composite membranes with very low thickness and good mechanical properties, whereas the manipulation of pristine Nafion® membranes becomes unpractical below a thickness of 50 μm.

The apparent methanol permeability has been distinguished from the true permeability property intrinsic to the membrane material. In this regard, the composite membranes showed a methanol permeability coefficient with one order of magnitude reduction in comparison to pristine Nafion®, as a consequence of the barrier effect caused by the nanofibers. However, the nanofiber phase does not seem to influence the electro-osmotic drag coefficient of methanol, although at certain conditions lower values were observed in the Nafion/PVA membranes. Interestingly, the electro-osmotic drag coefficient of methanol was found to decrease with temperature, as opposed to the water behaviour which has been reported to increase with increasing temperature.

Direct methanol fuel cell tests at different conditions of temperature and methanol concentration showed the maximum performances to be achieved at 95 °C and 2 M solutions. At those conditions, the Nafion/PVA membranes of 19 and 47 μm thickness reached equivalent performances to those of Nafion® membranes with comparable thickness, in spite of the higher protonic resistance found at the composite membranes.

The incorporation of a nanofiber phase within the Nafion® matrix and the use of thin membranes suggest that significant savings in the consumed amount of Nafion® polymer are able to be potentially afforded while keeping high performances.

Acknowledgements

This research is in the frame of IMIDIC/2009/155 project granted by Generalitat Valenciana through Institute for Small and Medium Industry (IMPIVA) and European Union by FEDER funds. The IMIDIC/2009/155 project belongs to the call for Technological Centres of IMPIVA Network.

References

[1] B. Smitha, S. Sridhar, A.A. Khan, J. Membr. Sci. 259 (2005) 10 (review).
[2] S. Tan, D. Bélanger, J. Phys. Chem. 109 (2005) 23480.
[3] D.H. Jung, S.Y. Cho, D.H. Peck, D.R. Shin, J.S. Kim, J. Power Sources 106 (2002) 173–177.
[4] M. Fujimura, T. Hashimoto, H. Kawai, Macromolecules 14 (1981) 1309.
[5] J. Müller, G. Frank, K. Colbow, D. Wilkinson, in: W. Vielstich, A. Lamm, H.A. Gasteiger (Eds.), Handbook of Fuel Cells—Fundamentals, Technology and Applications, vol. 3, Wiley, Chichester, 2003 (Chapter 62).

[6] M. Neergat, K.A. Friedrich, U. Stimming, Fuel Cells 2 (2002) 25–30.
[7] T. Shimizu, T. Naruhashi, T. Momma, T. Osaka, Electrochemistry 70 (2002) 991.
[8] C.-Y. Chen, J.I. Garnica-Rodriguez, M.C. Duke, R.F. Dalla Costa, A.L. Dicks, J.C. Diniz da Costa, J. Power Sources 166 (2007) 324.
[9] A. Sungpet, J. Membr. Sci. 226 (2003) 131–134.
[10] Q.M. Huang, Q.L. Zhang, H.L. Huang, W.S. Li, Y.J. Huang, J.L. Luo, J. Power Sources 184 (2008) 338–343.
[11] N. Li, J.Y. Lee, L.H. Ong, J. Appl. Electrochem. 22 (1992) 512.
[12] C. Barthet, M. Guglielmi, Electrochim. Acta 41 (1996) 2791.
[13] P. Aldebert, P. Audebert, M. Armand, G. Bidan, M. Pineri, Chem. Soc., Chem. Commun. (1986) 1636.
[14] S. Tan, A. Laforgue, D. Bélanger, Langmuir 19 (2003) 744.
[15] K.A. Mauritz, D.A. Mountz, D.A. Reuschle, R.I. Blackwell, Electrochim. Acta 50 (2004) 565–569.
[16] Q. Deng, Y. Hu, R.B. Moore, C.L. McCormick, K.A. Mauritz, Chem. Mater. 9 (1997) 36–44.
[17] N. Miyake, J.S. Wainright, R.S. Savinell, J. Electrochem. Soc. 148 (8) (2001) A905–A909.
[18] W.C. Choi, J.D. Kim, S.I. Woo, J. Power Sources 96 (2001) 411.
[19] Z.G. Shao, X. Wang, I.M. Hsing, J. Membr. Sci. 210 (2002) 147.
[20] D. Kreuer, Chem. Mater. 5 (1996) 610.
[21] J.F. Synder, M.A. Ratner, D.F. Shriver, Solid State Ionics 147 (2002) 249.
[22] S.J. Paddison, Annu. Rev. Mater. Res. 33 (2003) 289.
[23] H.-L. Lin, T.L. Yu, L.N. Huang, L.C. Chen, K.S. Shen, G.B. Jung, J. Power Sources 150 (2005) 11–19.
[24] V. Compañ, A. Andrio, A. López-Alemany, E. Riande, M.F. Refojo, Biomaterials 23 (2002) 2767–2772.
[25] S. Mollá, V. Compañ, J. Membr., to be published.
[26] C.-H. Ma, T. Leon Yu, H.-L. Lin, Y.-T. Huang, Y.-L. Chen, U.-S. Jeng, Y.-H. Lai, Y.-S. Sun, Polymer 50 (2009) 1764–1777.
[27] N.W. DeLuca, Y.A. Elabd, J. Membr. Sci. 282 (2006) 217–224.
[28] P. Mukoma, B.R. Jooste, H.C.M. Vosloo, J. Membr. Sci. 243 (2004) 293–299.
[29] D.W. Kim, H.-S. Choi, C. Lee, A. Blumstein, Y. Kang, Electrochim. Acta 50 (2004) 659–662.
[30] J.-C. Tsai, H.-P. Cheng, J.-F. Kuo, Y.-H. Huang, C.-Y. Chen, J. Power Sources 189 (2009) 958–965.
[31] J. Larminie, A. Dicks, Fuel Cell System Explained, John Wiley & Sons Ltd., Chichester, England, 2000 (Chapter 3).
[32] Z. Qi, A. Kaufman, J. Power Sources 110 (2002) 177–185.
[33] V.S. Silva, A. Mendes, L.M. Madeira, S.P. Nunes, J. Membr. Sci. 276 (2006) 126–134.
[34] G. Murgia, L. Pisani, A.K. Shukla, K. Scott, J. Electrochem. Soc. 150 (2003) A1231–A1245.
[35] K. Scott, W. Taana, J. Cruickshank, J. Power Sources 65 (1997) 159–171.
[36] L.-N. Huang, L.-C. Chen, L.T. Yu, H.-L. Lin, J. Power Sources 161 (2006) 1096–1105.
[37] L.-C. Chena, T.L. Yu, H.-L. Lin, S.-H. Yeh, J. Membr. Sci. 307 (2008) 10–20.
[38] Z. Luo, Z. Chang, Y. Zhang, Z. Liu, J. Li, Int. J. Hydrogen Energy 35 (2010) 3120–3124.